Analytical Methods

Analytical Methods

Advancing Methods and Applications

www.rsc.org/methods

RSC Publishing

PAPER
Russell et al.
Glycoprotein microarray for the fluorescence detection of antibodies produced as a result of erythropoietin (EPO) abuse

PAPER
Stefan-van Staden
Enantioanalysis of S-Ibuprofen using [5-(6)fullerene-C$_{60}$ and diethyl (1,2-methanofullerene C$_{60}$)-71-71-dicarboxylate

1759-9660(2010)2:1;1-A

1   **L-cysteine/Glycine composite film modified glassy carbon electrode as enhanced**

2   **sensing platform for catechol determination**

3

4   **Jiahong He[a,b,c], Shaohua Xing[b], Ri Qiu[b], Zhongrong Song[c], Shengtao Zhang[a]***

5   a   School of Chemistry and Chemical Engineering, Chongqing University,

6   Chongqing 400044, P. R. China

7   b Science and Technology on Marine Corrosion and Protection Laboratory, Luoyang

8   Ship Material Research Institute, Qingdao 266101, P. R. China

9   c School of Materials and Chemical Engineering, Chongqing University of Arts and

10   Sciences, Yong chuan 402160, P. R. China

11

12

13

14

15

16

17

18

19

20

21

* Corresponding author. Tel: +86-23-65102531.

Email: stzhang@cqu.edu.cn; 20110901036@ cqu.edu.cn

22   **Abstract**

23   In this report, a novel voltammetric sensor based on a glassy carbon electrode

24   modified with L-cysteine/glycine composite film (L-cysteine/glycine/GCE) was

25   developed for the quantitative detection of catechol. The as-fabricated electrode

26   exhibited good electrochemical performance with low electron transfer resistance.

27   The results of electrochemical impedance spectroscopy (EIS) revealed that

28   electron transfer through L-cysteine/glycine film was more facile than that of the

29   bare glassy carbon electrode. The electrochemical behavior of catechol was also

30   investigated by cyclic voltammetry (CV) and differential pulse voltammetry (DPV)

31   at the prepared electrode. The modified electrode showed excellent electrocatalytic

32   activity towards the oxidation of catechol in $NaOH-KH_2PO_4$ buffer solution

33   (pH=6.0). Under the optimum conditions, the linear relationship between the

34   oxidation peak current and concentration of catechol can be obtained in the range

35   from 3 μM to 280 μM with the detection limit as 0.32 μM (3σ). In addition, the

36   interference and stability study showed a satisfactory detection result by this

37   electrode. Besides, the proposed method was successfully applied to the

38   determination of catechol in water samples with satisfactory results.

39   **Keywords**

40   Glycine; L-cysteine; Catechol; Electrocatalysis; Sensor

41

42

43

44   **1. Introduction**

45   As an essential industrial raw material, catechol is widely used in rubber, dyes,

46   plastics, pesticides, flavoring agents, antioxidant, leather tanning, photography and

47   other synthetic chemical industries [1-2]. Thus, it can be easily introduced into the

48   environment as pollutant. Moreover, catechol is highly toxic to living beings. McCue

49   et al. [3] found that cigarette tar contained a trace amount of catechol, which could

50   induce damage to DNA and cause cancer to humans [4-5]. Due to its extreme

51   harmfulness to creatures even at very low concentration, the US Environmental

52   Protection Agency (EPA) and the European Union (EU) consider catechol as an

53   environmental pollutant [6-7]. In the national standard (GB 8978-1996) of China, the

54   permitted emission concentration of phenolic compounds is regulated as 0.5 mg/L

55   (for dihydroxybenzene, 4.54×10^{-3} M) [8]. With the increasing demand in the

56   environmental protection and public safety, the determination of this toxicity has

57   received much attention. Up to now, several methods have been devoted for the

58   determination of catechol, such as chemiluminescence [9-10], spectrophotometry

59   [11-12], high performance liquid chromatography (HPLC) [13-14], fluorescence

60   quenching method [15], electro-chemiluminescent [16], and H-point curve isolation

61   method [17]. Although these methods have been successfully applied to catechol

62   determination, they still suffer from some drawbacks such as complex operating

63   conditions, time-consuming processes, expensive equipments, and so forth.

64   Electrochemical method is a promising technique for the determination of the small

65   organic compounds in aqueous solution due to its advantages of fast response, cheap

66   instrument, low cost, simple operation, high sensitivity and excellent selectivity. In

67   recent years, many efforts have been paid to the electrochemical determination of

68   catechol at different electrodes. For example, based on cyclic voltammetry and

69   differential pulse voltammetry methods, Deng et al. [18] detected catechol by using

70   gold nanoparticle/sulfonated graphene modified electrode. Compared with graphene

71   modified electrode, the composite modified one exhibited obvious desorption

72   properties toward aromatic species of catechol, and the results illustrated that the

73   sensor displayed high chemical selectivity, fast response and good reproducibility to

74   low concentration of catechol. Wang et al. [19] reported a gold nanoparticles/TiO_2

75   composite modified indium tin oxide (ITO) electrode to study the electrochemical

76   behavior of catechol using cyclic voltammetry and differential pulse voltammetry

77   techniques. The proposed sensor was applied to determine catechol in tea samples,

78   and the results were satisfactory compared with the chromatography approach.

79   Besides, Zheng et al. [20] prepared polydopamine (PDA)-reduced graphene oxide

80   (RGO) nanocomposite electrode by one-step procedure. Their research showed that

81   the PDA-RGO modified electrode exhibited high electrocatalytic activity toward the

82   oxidation of catechol and the electrode was successfully applied to the determination

83   of catechol in tap water samples with excellent stability, reproducibility and

84   selectivity. In addition, other modified electrodes such as GO-MnO_2/GCE [21],

85   GMC/GCE [22], EGE/MMT [23], ECF/CPE [24], and MWNTs-IL-Gel/GCE [25],

86   also emerged for catechol determination. Although these sensors have good

87   electrochemical performances, their preparation process is usually complex, which

88   may play the hurdle for their practical application.

89   In this paper, we chose cheap and environmentally friendly glycine and L-cysteine as

90   modification materials to fabricate a novel L-cysteine/glycine/GCE. The

91   electrochemical behavior of catechol on L-cysteine/glycine/GCE was investigated. It

92   was found that the modified electrode exhibited excellent electrocatalytic activity

93   towards the oxidation of catechol, and the oxidation peak current was linear to

94   catechol concentration in a certain range. To the best of our knowledge, this is the

95   first time that such high sensitivity has been achieved for the detection of catechol

96   using L-cysteine/glycine modified electrode.

97

98   **2. Experimental**

99   **2.1 Apparatus and reagents**

100   Electrochemical experiments were performed on a CHI660D electrochemical

101   workstation (Shanghai Chenhua Co., Ltd., China) cabled with a conventional

102   three-electrode cell. A bare or modified GCE was used as the working electrode, and

103   a platinum wire electrode was applied as the auxiliary electrode. A saturated calomel

104   electrode (SCE) worked as the reference electrode. If there is no specific indication,

105   all potentials reported in this paper are quoted with SCE. Electrochemical impedance

106   spectroscopy (EIS) measurements were conducted using PARSTAT2273 (EG&G,

107   USA). An S-2F digital pH meter (Leici instrument factory, Shanghai, China) was

108   used to determine pH of buffer solution.

109   All reagents were obtained as analytical grade and used without further purification.

110   Doubly distilled water obtained from a Milli-Q water purification system

111   (18MΩ•cm) was for all experiments. Catechol was purchased from Sinopharm

112   Chemical Reagent Beijing Co., Ltd. Glycine and L-cysteine were obtained from

113   Shanghai Kangda Amino Acid Company.

114   **2.2 Preparation of modified electrode**

115   Scheme 1 illustrates the procedure for the fabrication of L-cysteine/glycine onto

116   GCE. Firstly, prior to the electrodeposition of glycine and L-cysteine, GCE (Φ=3mm)

117   was polished repeatedly with 0.3 and 0.05 μm alumina powder. Then, it was

118   successively sonicated in nitric acid (1:1), acetone, ethanol and doubly distilled

119   water for 5 min and dried at room temperature. Secondly, GCE was immersed into

120   0.01 M glycine solution (NaOH-KH$_2$PO$_4$ buffer, pH=6.0), and cyclic voltammetry

121   was used to deposit glycine onto GCE surface. The potential range was selected as

122   -0.5 ~ 1.5 V with the sweeping rate 100 mV/s, and the sweeping cycle number was

123   16. The solution was deoxygenated for 20 min with nitrogen prior to

124   electrodeposition. Thirdly, in an aqueous solution containing 0.01 M L-cysteine

125   (NaOH-KH$_2$PO$_4$ buffer solution, pH 6.0), L-cysteine was electrodeposited by cyclic

126   voltammetry in a potential range of -0.8 ~ 0.6 V for 8 cycles with the sweeping rate

127   of 100 mV/s.

128

129   **Preferred position for Scheme 1.**

130

131   **2.3 Morphology and electrochemical property of the electrodes.**

6

132 The surface morphology was revealed by a field emission scanning electron

133 microscopy (FE-SEM, Zeiss Ultra 55). The electrochemical property of the

134 electrodes were evaluated on CHI 660D electrochemical workstation in a

135 conventional three-electrode cell. High-purity nitrogen was used for purging oxygen

136 before each experiment. The measurements were carried out at ambient temperature

137 (25 ± 2 ^{o}C). The electrochemical performance of L-cysteine/glycine/GCE was

138 measured by cyclic voltammetry (CV) and differential pulse voltammetry (DPV) in

139 buffer solution (NaOH-KH_2PO_4, pH= 6.0) in the potential range of -0.2 ~ 0.6 V with

140 the scan rate 100 mV/s. Besides, the electrochemical impedance spectroscopy was

141 performed in 5 mM $Fe(CN)_6^{3-/4-}$ solution containing 0.1 M KCl and the frequency

142 range was from 0.01 to 10^5 Hz.

143 **3. Results and discussion**

144 **3.1 Electrode preparation**

145 To determine the electrodepostion order during the preparation of the electrode,

146 glycine /L-cysteine/ GCE and L-cysteine/glycine/GCE were prepared to compare the

147 electrochemcial activity to catechol. Fig. 1 shows the CV curves of catechol at the

148 two electrodes in the potential range of -0.2 V to +0.6 V. The employed scan rate is

149 50 mV/s. For glycine/L-cysteine/GCE (curve a), the redox peaks of cathodic shown

150 at 0.318 V and -0.053 V, and the peak-to-peak ($\Box E_p$) value is calculated as 0.371 V.

151 Curve b is the CV of L-cysteine/glycine/GCE. A pair of redox peaks can be observed

152 with the anodic peak potential as 0.148 V and the cathodic peak potential as 0.007 V.

153 $\Box E_p$ value is calculated as 0.141 V. Compared with Curve a, the peak currents of

154   Curve b have increased remarkably. The further decrease of $\Box E_p$ value and the

155   increase of redox peak currents demonstrate that the L-cysteine/glycine/GCE has

156   better performance for the cathodic determination of catechol. In this study, we select

157   L-cysteine/glycine/GCE as the representative for catechol determination.

158

159   **Preferred position for Fig. 1**

160

161   The L-cysteine/glycine film was fabricated through two steps. In the first step, the

162   CV curves to immobilize glycine onto GCE surface are shown as Fig. 2a. During the

163   electrodeposition process, it is clear that an oxidation peak is observed at 0.96 V

164   during the anodic scan. Two reduction peaks appears at 0.45 V and -0.13 V in the

165   reverse reduction scan due to the formation of glycine film. During the electrode

166   reaction, glycine molecules are oxidized to free radicals. By combining with the

167   GCE surface rapidly (Scheme 2), glycine will finally immobile on the electrode

168   surface. After that, L-cysteine was further electrodeposited onto the as-form

169   glycine/GCE surface to reach L-cysteine/glycine/GCE state. The CV curves during

170   electrodeposition of L-cysteine are shown as Fig. 2b. A reduction peak appears at

171   -0.63 V during the reduction scan. The reduction peak current enhances with the

172   increment of the cycle number. It is assumed the reaction indicated in Scheme 3

173   occurs during the electrodeposition process:

174   **Preferred position for Fig. 2**

175

176   **Preferred position for Scheme 2.**

8

177   **Preferred position for Scheme 3.**

178

179   For further confirmation of the achievement of L-cysteine/glycine/GCE during the

180   two step protocol, SEM technique is employed to reveal the surface morphology of

181   glycine/GCE, L-cysteine/GCE and L-cysteine/glycine/GCE, which are shown as Fig.

182   3. It is found that the external shape of as-deposited glycine and L-cysteine is quite

183   different. After two-step-procedure to realize L-cysteine/glycine/GCE, the surface is

184   similar to the L-cysteine/GCE, since L-cysteine acts as the "external shell" in the

185   composite film. With the SEM images, it is demonstrated that L-cysteine/glycine

186   composite has been formed on GCE surface. The composite surface behaves as a

187   highly rough structure, which increases the specific surface area of the electrode.

188   With this structure, the diffusion of the ions or target molecules to the electrode will

189   be promoted, so that a high catalytic capability will be obtained.

190   **Preferred position for Fig. 3**

191

192   **3.2 Electrochemical impedance spectroscopy measurement.**

193   Electrochemical impedance spectroscopy (EIS) is a powerful and non-destructive

194   method to study electrochemical property of solid/liquid interface [26]. In this report,

195   EIS measurements were carried through by using 5.0 mM $Fe[(CN)_6]^{3-/4-}$ as the redox

196   probe, and the results are shown in Fig. 4. The diameter of the semicircle is

197   equivalent to the charge transfer resistance (R_{ct}), which is the direct and sensitive

198   parameter corresponding to chemical reaction near the electrode-solution interface

9

199   [27]. It can be observed that the semicircle diameter of the L-cysteine/glycine/GCE

200   is smaller than that of the bare GCE, L-cysteine/GCE and glycine /GCE, suggesting

201   that the charge transfer rate of GCE modified with L-cysteine/glycine composite film

202   is much faster than other electrodes. Also, it is indicated that L-cysteine/glycine

203   composite film has been successfully modified on GCE.

204

205   **Preferred position for Fig. 4**

206

207   **3.3 Electrochemical behavior of catechol at modified GCE**

208   The electrochemical behavior of catechol at various modified electrodes has been

209   studied by CV. Fig. 5 shows the CV response of catechol on various electrodes in the

210   potential range of -0.2 V to + 0.6 V in buffer solution (NaOH-KH$_2$PO$_4$, pH=6.0). In a

211   blank buffer solution (Curve a), L-cysteine/glycine/GCE shows no redox peaks due

212   to the absence of catechol. On bare GCE (curve b), a pair of broad redox peaks can

213   be observed with the anodic peak potential (E$_{pa}$) as 0.512 V and the cathodic peak

214   potential (E$_{pc}$) as -0.016 V. The peak-to-peak separation ($\triangle$E$_p$) value is calculated as

215   0.528 V, indicating that catechol exhibits an irreversible electrochemical behavior at

216   bare GCE [28-29]. On glycine/GCE (curve c) and L-cysteine/GCE (curve d), the

217   redox peaks of catechol are shown at 0.276/-0.042 V and 0.224/-0.028 V,

218   respectively. The $\triangle$E$_p$ values decrease to 0.318 V and 0.252 V, and the redox peak

219   currents increase, illustrating that both glycine and L-cysteine can act as effective

220   mediators during the electrocatalytic oxidation of catechol. When combining both

10

221   mediators together to form L-cysteine/glycine/GCE (curve e), a pair of well-defined

222   redox peaks are observed with ΔE_p value as 0.138 V. Also, the enhanced anodic and

223   cathodic peak currents, i. e., -37.354 µA and 30.294 µA, can be observed. The

224   decrease of the ΔE_p value and the increase of redox peak currents demonstrate that

225   L-cysteine/glycine film acts as an efficient promoter to enhance the kinetics of

226   electrochemical process, which is probably attributed to the synergistic

227   electrocatalysis effect of L-cysteine and glycine. The results indicate that the

228   L-cysteine/glycine composite film modified electrode is qualified for the

229   determination of catechol.

230

231   **Preferred position for Fig. 5**

232

233   The excellent performance of L-cysteine/glycine/GCE can be attributed to the

234   following reasons. Firstly, as shown in Scheme 4, the amino, carboxyl, and

235   sulfhydryl group in glycine and L-cysteine can interact with the hydroxyl groups of

236   catechol via H-bonding. In the buffer solution (pH=6.0), the negatively charged

237   L-cysteine/glycine composite film can interact with the positively charged catechol

238   (pK_a = 9.40 [30]) through the favorable electrostatic attraction, which helps to lower

239   activation energy required during the redox reactions, so that the overpotential for

240   the reaction will be decreased [31]. Secondly, the L-cysteine/glycine/GCE surface is

241   intrinsically rough, so that a high specific surface area makes the enrichment of

242   catechol easily. With the EIS experiments, it is also demonstrated that the charge

243   transfer kinetics of L-cysteine/glycine/GCE is fast. Therefore, the redox reaction of

244   catechol on L-cysteine/glycine/GCE is accelerated.

245

246   **Preferred position for Scheme 4**

247

248   **3.4 pH effect on CV behavior of the sensor**

249   Electrolyte acidity affects electro-oxidation behavior of catechol, because proton

250   participates in the electrode reaction [31]. In this work, the voltammetric behavior of

251   catechol in different electrolyte solutions, i. e., KH_2PO_4-Na_2HPO_4 (PBS), HAc-NaAc,

252   NaOH-KH_2PO_4, Britton-Robinson buffer solution (B-R) are investigated. The results

253   indicate that NaOH-KH_2PO_4 buffer solution has the best effect on the

254   electro-oxidation behavior of catechol. Thus, we choose NaOH-KH_2PO_4 buffer

255   solution as the electrolyte.

256   On L-cysteine/glycine/GCE, pH effect on peak potentials and peak currents of

257   catechol are carefully investigated by CV. As shown in Fig. 6A, it is observed that

258   the oxidation peak current of catechol increases with the enhancement of pH value

259   until it reaches 6.0. After that, the current decreases slightly. Liu, et al. [32] proposed

260   that the electrostatic repulsion between the electrode and the target molecules could

261   be the most possible reason for this phenomenon. Also, other two important reasons

262   should be taken into consideration [8, 33-34]. Firstly, the solution with high pH

263   value is not advantageous to electrochemical reaction due to the shortage of proton;

264   Secondly, catechol molecule has proton in its own structure, which can easily

265   undergo deprotonation and turn into anions in high pH aqueous solution. Meanwhile,

266   glycine and L-cysteine on electrode surface are also negatively charged due to the

267   further dissociation of carboxyl and sulfhydryl group. Consequently, the electrostatic

268   repulsion between catechol and electrode will be enhanced with the increase of pH

269   value, which leads to low adsorption capacity on the electrode surface and low peak

270   current. Hence, pH of 6.0 has been chosen as the optimum acidity for further

271   experiments.

272   As shown in Fig. 6B, the relationship between the peak potential and pH is also

273   investigated. It is found that peak potential shifts negatively with the increase of pH.

274   Two linear relationship are obtained with the regression equations of E_{pa} (V) =

275   -0.0633 pH + 0.5553 (R = 0.9958) for oxidation process and E_{pc} (V) = -0.0672 pH +

276   0.3192 (R = 0.9963) for reduction process. According to the formula dEp/dpH =

277   2.303mRT/nF [35], in which m and n are the number of proton and electron, for

278   catechol oxidation process, m/n was calculated as 1.07. It indicates that the number

279   of proton is same to that of the electron involved in the redox process of catechol.

280

281   **Preferred position for Fig. 6**

282

283   **3.5 Effect of the scan rate on the electrochemical behavior of catechol**

284   For   further   understanding   electrochemical   behavior   of   catechol   at   the

285   L-cysteine/glycine/GCE, the influence of scan rate is examined. As shown in Fig. 7,

286   both cathodic and anodic peak current (I_{pc} and I_{pa}) of catechol are linear to the square

287   root of scan rate in the range of 20 ~ 130 mV/s. The redox peak currents follow the

288   linear regression equation of I_{pa} = -3.5751 $\upsilon^{1/2}$ + 5.1731 (μA, mV/s, R = 0.9984) and

289   I_{pc} = 3.3723 $\upsilon^{1/2}$ - 6.9117 (μA, mV/s, R = 0.9984), indicating that the electrode

290   process of catechol is a diffusion-controlled process [36-38]. Besides, from Fig. 7, it

291   can also be seen that E_{pa} shifts to more positive values along with the increase of the

292   scan rate. These results illustrate that the electron transfer is quasi-reversible [39].

293

294   **Preferred position for Fig. 7**

295

296   **3.6 Effect of cycle number during L-cysteine/glycine deposition on GCE**

297   The as-grown film thickness is essentially dependent on the cycle number of CV

298   during the electrodeposition process [40]. In this report, the dependent relationship

299   between CV cycle number for L-cysteine/glycine deposition and catechol redox

300   ability is also studied. Fig. 8 (A) and (B) illustrate the variation of electrochemical

301   behavior toward to catechol on L-cysteine/glycine/GCE with different cycle numbers

302   of L-cysteine/glycine films. In Fig. 8 (A), when the cycle number of glycine and

303   L-cysteine deposition adopts 16 and 8, E_{pa} and E_{pc} reach the minimum and

304   maximum value, respectively. At the same time, the oxidation peak currents of

305   catechol also arrive at a maximum value in the same case (Fig. 8 (B)). Moreover,

306   when the cycle number increases further, the electrochemical activity of

307   L-cysteine/glycine film will decrease. Since the as-achieved thick film has high

308   impedance, it is hard for electrons to penetrate through to reach the electrode surface

14

309   [41]. In other words, a very thick or thin film is not beneficial for electrode response.

310   Only optimum thickness originated from the reasonable CV cycle number (16 cycles

311   for glycine and 8 cycles for L-cysteine) can enable the lowest ΔE_p and the highest

312   sensitivity.

313

314   **Preferred position for Fig. 8**

315

316   **3.7 The response characteristics of the sensor to catechol**

317   The amperometric responses are measured at the bare GCE, glycine/GCE,

318   L-cysteine/GCE and L-cysteine/glycine/GCE. During the experiments, the potential

319   of 0.148 V is exerted onto the electrodes. At this potential, amperometric response

320   reaches a maximum value (Fig. 5). Therefore, the typical current-time curves are

321   obtained by plotting the reaction time against the corresponding current (Fig. 9). As

322   illustrated, the sensor rapidly responds and reaches a steady state within a short time

323   after the addition of catechol into the solution, demonstrating the high sensitivity to

324   catechol. This phenomenon can be attributed to the well-defined surface area of

325   electrode [42]. Furthermore, drastic increase in the responsive current is observed at

326   the L-cysteine/glycine/GCE with the addition of the catechol. However,

327   glycine/GCE, L-cysteine/GCE and bare GCE show relatively small current response

328   to catechol. L-cysteine/glycine/GCE behaves faster response and higher sensitivity

329   than other electrodes due to the synergistic effect between glycine and L-cysteine.

330

331   **Preferred position for Fig. 9**

332

333   **3.8 Interference of coexisting substances**

334   In order to evaluate the selectivity of the proposed method for catechol

335   determination, the effect of various foreign species is also investigated. The

336   tolerance limit is taken as the maximum concentration of the foreign substances

337   causing an approximately ±5% relative error in their determination. The results show

338   that 500-fold concentration of Na^+, K^+, NH_4^+, NO_3^-, 300-fold concentration of Ca^{2+},

339   Mg^{2+}, Cu^{2+}, Al^{3+}, Fe^{2+}, SO_4^{2-} and 100-fold concentration of ascorbic acid, phenol,

340   resorcinol do not show interference to the detection of 50 μM catechol. However,

341   20-fold concentration of hydroquinone disturbs the determination. It is confirmed

342   that the as-modified electrode performs good selectivity.

343   **3.9 Analytical property characterization**

344   The linear range and detection limitation are studied using DPV under the optimum

345   conditions. The DPV responses for various concentration of catechol are illustrated

346   in Fig. 10. With the increase of catechol concentration, the oxidation peak current

347   linearly enhances to the concentration of catechol in the range of 3 ~ 280 μM. The

348   linear equation is I_{pa} (μA) = -12.3153 + 0.2613C (μM) with a correlation coefficient

349   of 0.9981. The detection limit is 0.32 μM (3σ). Compared with other modified

350   electrodes reported previously, the as-prepared L-cysteine/glycine/GCE in this work

351   behaves superior electroanalysis property (listed in Table.1).

352

353   **Preferred position for Fig. 10**

354   **Preferred position for Table 1**

355

356   **3.10 Stability and reproducibility of the modified electrode**

357   Good reproducibility and stability are considered as two key criteria for judging a

358   sensor [51]. Under the optimal conditions, the reproducibility of the amperometric

359   sensor is evaluated by successive determination (n=8) of catechol (50 μM), and the

360   relative standard deviation (RSD) is calculated as 1.39%. The fabrication

361   reproducibility is also estimated with five different electrodes, which are fabricated

362   independently by the same procedure. The RSD is 4.36% for measuring the peak

363   current in a 50 μM catechol solution, which demonstrates the reliability of the

364   fabrication procedure. For the stability evaluation of the modified electrode, when

365   the electrode is kept at 4 ^{o}C for two weeks, the peak currents retain more than 92.9%

366   of the initial values. The results reveal that the as-modified electrode presents a good

367   repeatability and durability.

368   **3.11 Samples analysis**

369   In order to assess the applicable capability of this method for the determination of

370   catechol, local tap water samples without any pretreatment are used for quantitative

371   analysis. Standard solutions of catechol are added into the water sample. The catechol

372   is then determined by DPV method. The results are summarized in Table 2. The

373   recoveries of the samples range between 99.2% and 102.6%, and these results clearly

374   indicate the reliability of the method.

17

375

Preferred position for Table 2

377

378   **4. Conclusions**

379   (1) Electrodeposition is proven applicable to obtain L-cysteine/glycine composite

380   film onto GCE surface.

381   (2) L-cysteine/glycine composite film exhibits electrocatalytic activity to catechol

382   oxidation. Well-defined oxidation peaks with lower anodic overpotential and the

383   significantly   increased   peak   current   of   catechol   are   observed   at

384   L-cysteine/glycine/GCE.

385   (3) A plausible mechanism for catechol electrocatalysis has been demonstrated.

386   (4) L-cysteine/glycine/GCE has been employed as a sensor for determination of

387   catechol. High sensitivity, good stability, wide linear range and reproducibility

388   enable it as a new potential candidate for catechol determination.

394

395   **References**

396   [1] H. Zhang, J. S. Zhao, H. T. Liu, R. M. Liu, H. S. Wang, J. F. Liu, Microchim.

397   Acta, 2010, 169, 277-282.

398   [2] B. Unnikrishnan, P. L. Ru, S. M. Chen, Sens. Actuators, B, 2012, 169, 235-242.

399   [3] J. M. McCue, K. L. Link, S. S. Eaton, B. M. Freed, J. Immunol, 2000, 165,

400   6771-6775.

401   [4] K. Hirakawa, S. Oikawa, Y. Hiraku, I. Hirosawa, S. Kawanishi, Chem. Res.

402   Toxicol, 2002, 15, 76-82.

403   [5] N. Schweigert, J. L. Acero, U. V. Gunten, S. Canonica, A. J. B. Zehnder, R. I. L.

404   Eggen, Environ. Mol. Mutagen, 2000, 36, 5-12.

405   [6] T. Y. Xie, Q. W. Liu, Y. R. Shi, Q. Y. Liu, J. Chromatogr A, 2006, 1109, 317-321.

406   [7] S. Timur, N. Pazarlioglu, R. Pilloton, A. Telefoncu, Talanta, 2003, 61, 87-93.

407   [8] H. S. Yin, Q. M. Zhang, Y. L. Zhou, Q. Ma, T. Liu, L. S. Zhu, S. Y. Ai,

408   Electrochim. Acta, 2011, 56, 2748-2753.

409   [9] L. J. Zhao, B. Q. Lv, H. Y. Yuan, Z. D. Zhou, D. Xiao, Sensors, 2007, 7, 578-588.

410   [10] S. F. Li, X. Z. Li, J. Xu, X. W. Wei, Talanta, 2008, 75, 32-37.

411   [11] P. Nagaraja, R.A. Vasantha, K.R. Sunitha, Talanta, 2001, 55, 1039-1046.

412   [12] E. C. Figueiredo, C. R. T. Tarley, L. T. Kubota, S. Rath, M. A. Z. Arruda,

413   Microchem. J., 2007, 85, 290-296.

414   [13] G. Marrubini, E. Calleri, T. Coccini, A. F. Castoldi, L. Manzo, Chromatographia,

415   2005, 62, 25-31.

416   [14] A. Asan, I. Isildak, J. Chromatogr., A, 2003, 988, 145-149.

417   [15] W. J. Dong, J. P. Song, C. Dong, M. M. F. Choi, Chinese Chem. Lett., 2010, 21,

418   346-348.

419   [16] Y. G. Sun, H. Cui, Y. H. Li, X. Q. Lin, Talanta, 2000, 53, 661-666.

420   [17] M. Hasani, M. Mohammadi, M. S. Rad, H. Abdollahi, Spectrochim acta a, 2012,

421   96, 563-568.

422   [18] D. H. Deng, S. J. Li, M. J. Zhang, X. N. Liu, M. M. Zhao, L. Liu, Anal.

423   Methods, 2013, 5, 2536-2542.

424   [19] G. F. Wang, X. P. He, F. Zhou, Z. J. Li, B. Fang, X. J. Zhang, L. Wang, Food

425   Chem., 2012, 135, 446-451.

426   [20] L. Z. Zheng, L. Y. Xiong, Y. D. Li, J. P. Xu, X. W. Kang, Z. J. Zou, S. M. Yang,

19

427   J. Xia, Sens. Actuators, B, 2013, 177, 344-349.

428   [21] T. Gan, J. Y. Sun, K. J. Huang, L. Song, Y. M. Li, Sens. Actuators, B, 2013, 177,

429   412-418.

430   [22] S. K. Lunsford, H. Choi, J. Stinson, A. Yeary, D. D. Dionysiou, Talanta, 2007,

431   73, 172-177.

432   [23] Y. Kong, Y. Y. Xu, H. H. Mao, C. Yao, X. F. Ding, J. Electroanal. Chem., 2012,

433   669, 1-5.

434   [24] Q. H. Guo, J. S. Huang, P. Q. Chen, Y. Liu, H. Q. Hou, T. Y. You, Sens.

435   Actuators, B, 2012, 163, 179-185.

436   [25] C. H. Bu, X. H. Liu, Y. J. Zhang, L. Li, X. B. Zhou, X. Q. Lu, Colloids Surf., B,

437   2011, 88, 292-296.

438   [26] B. W. Park, D. Y. Yoon, D. S. Kim, J. Electroanal. Chem., 2011, 661, 329-335.

439   [27] D. M. Zhao, X. H. Zhang, L. J. Feng, L. Jia, S. F. Wang, Colloids Surf., B, 2009,

440   74, 317-321.

441   [28] A. J. S. Ahammad, S. Sarker, M. A. Rahman, J. J. Lee, Electroanal., 2010, 22,

442   694-700.

443   [29] P. Yang, Q. Y. Zhu, Y. H. Chen, F. W. Wang, J. Appl. Polym. Sci., 2009, 113,

444   2881-2886.

445   [30] A. J. S. Ahammad, M. M. Rahman, G. R. Xu, S. Kim, J. J. Lee, Electrochim.

446   Acta, 2011, 56, 5266-5271.

447   [31] K. Nakano, K. Ohkubo, H. Taira, M. Takagi, N. Soh, T. Imato, J. Electroanal.

448   Chem., 2008, 623, 49-53.

449   [32] W. L. Liu, C. Li, L. Tang, A. Y. Tong, Y. Gu, R. Cai, L. Zhang, Z. Q. Zhang,

450   Electrochim. Acta, 2013, 88, 15-23.

451   [33] H. J. Du, J. S. Ye, J. Q. Zhang, X. D. Huang, C. Z. Yu, J. Electroanal. Chem.,

452   2011, 650, 209-213.

453   [34] J. T. Han, K. J. Huang, J. Li, Y. M. Liu, M. Yu, Colloids Surf., B, 2012, 98,

454   58-62.

455   [35] E. Laviron, Adsorption, J. Electroanal. Chem. 1974, 52, 355-393.

456   [36] W. Sun, Y. Z. Li, M. X. Yang, J. Li, K. Jiao, Sens. Actuators, B, 2008, 133,

457   387-392.

458   [37] X. M. Ma, Z. N. Liu, C. C. Qiu, T. Chen, H. Y. Ma, Microchim. Acta, 2013, 180,

459   461-468.

460   [38] Z. M. Liu, Z. L. Wang, Y. Y. Cao, Y. F. Jing, Y. L. Liu, Sens. Actuators, B, 2011,

461   157, 540-546.

462   [39] X. L. Yuan, D. S. Yuan, F. L. Zeng, W. J. Zou, F. Tzorbatzoglou, P. Tsiakarasb, Y.

463   Wang, Appl catal b-environ., 2013, 129, 367-374.

464   [40] C. Y. Lumibao, L. M. V. Tillekeratne, J. R. Kirchhoff, D. M. D. Fouchard, R.

465   A. Hudson, Electroanalysis, 2008, 20, 2177-2184.

466   [41] W. M. Si, W. Lei, Y. H. Zhanga, M. Z. Xia, F. Y. Wang, Q. L. Hao, Electrochim.

467   Acta, 2012, 85, 295-301.

468   [42] D. H. Yuan, S. H. Chen, F. X. Hu, C. Y. Wang, R. Yuan, Sens. Actuators, B,

469   2012, 168, 193-199.

470   [43] Z. A. Xu, X. Chen, X. H. Qu, S. J. Dong, Electroanalysis, 2004, 16, 684-687.

471   [44] S. Tembe, S. Inamdar, S. Haram, M. Karve, S. F. D. Souza, J. Biotechnol., 2007,

472   128, 80-85.

473   [45] Y. Umasankar, A. P. Periasamy, S. M. Chen, Anal. Biochem., 2011, 411, 71-79.

474   [46] A. S. Kumar, P. Swetha, K. C. Pillai, Anal. Methods, 2010, 2, 1962-1968.

475   [47] B. P. Lopezab, A. Merkoci, Analyst, 2009, 134, 60-64.

476   [48] M. G. Li, F. Ni, Y. L. Wang, S. D. Xu, D. D. Zhang, S. H. Chen, L. Wang,

477   Electroanalysis, 2009, 21, 1521-1526.

478   [49] X. G. Kong, X. Y. Rao, J. B. Han, M. Wei, X. Duan, Biosens Bioelectron, 2010,

479   26, 549-554.

480   [50] L. Su, L. Q. Mao, Talanta, 2006, 70, 68-74.

481   [51] S. Y. Zhu, H. J. Li, W. X. Niu, G. B. Xu, Biosens. Bioelectron., 2009, 25,

482   940-943.

<div align="center">○ Glycine   ○ L-cysteine</div>

1
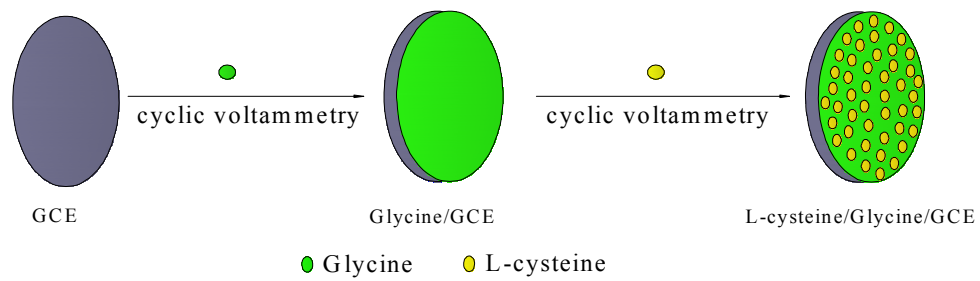
2   **Scheme 1.** The modification procedure to get the target electrode.
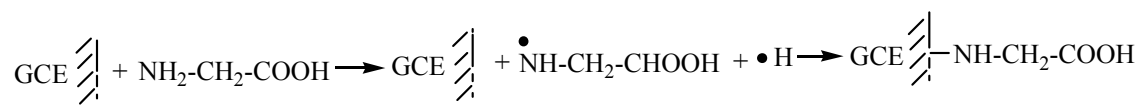
3

4
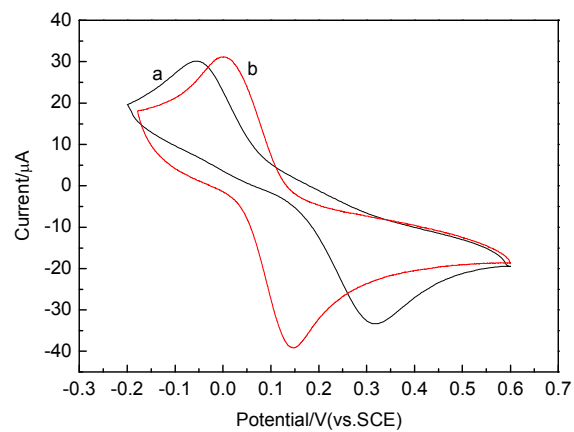
Fig. 1. CV curves of (a) glycine/L-cysteine/GCE and (b) L-cysteine/glycine/GCE in

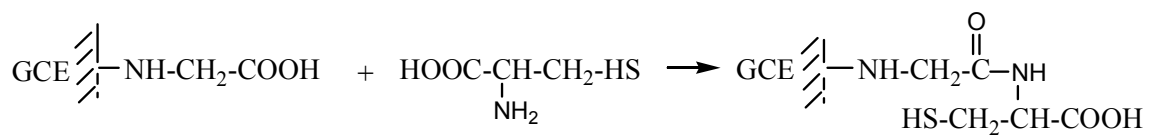NaOH-KH$_2$PO$_4$ buffer solution containing 50 µM catechol (scan rate: 50 mV/s).

9

10 $$\text{GCE} \diagup\!\!\!\!\big| + \text{NH}_2\text{-CH}_2\text{-COOH} \longrightarrow \text{GCE} \diagup\!\!\!\!\big| + \overset{\bullet}{\text{N}}\text{H-CH}_2\text{-CHOOH} + \bullet\,\text{H} \longrightarrow \text{GCE} \diagup\!\!\!\!\big|\!-\text{NH-CH}_2\text{-COOH}$$

11 **Scheme 2.** The immobilization mechanism of glycine onto GCE.

12

$$GCE-NH\text{-}CH_2\text{-}COOH \quad + \quad HOOC\text{-}CH\text{-}CH_2\text{-}HS \quad \longrightarrow \quad GCE-NH\text{-}CH_2\text{-}\overset{\displaystyle O}{\overset{\|}{C}}\text{-}NH$$

with NH_2 on the second reactant and $HS\text{-}CH_2\text{-}CH\text{-}COOH$ on the product.

13

14   **Scheme 3.** The immobilization procedure of L-cysteine onto glycine/GCE.
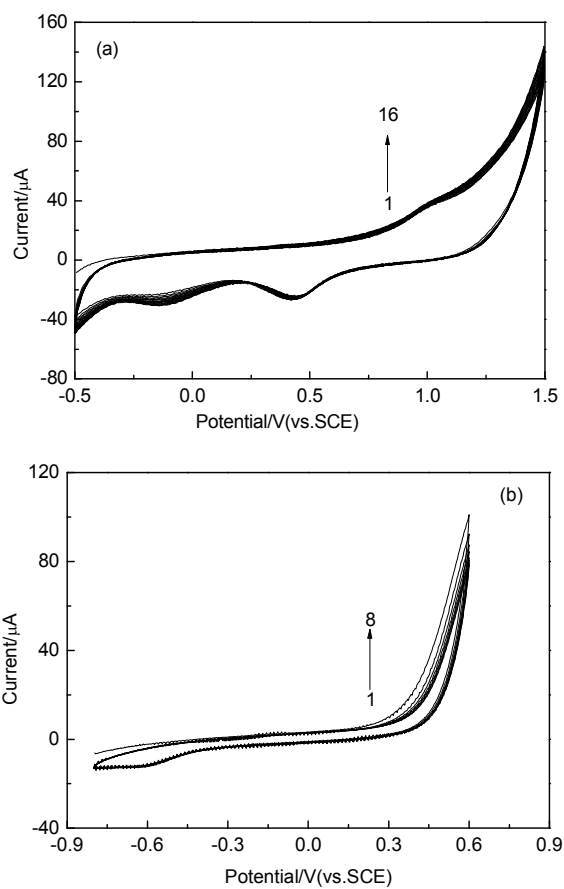
15

16

17   Fig. 2. CV curves during the electrodeposition (a) glycine and (b) L-cysteine on GCE with

18   scan rate 100 mV/s. The solutions are 0.01 M glycine or L-cysteine in NaOH-KH$_2$PO$_4$ buffer

19   solution (pH 6.0).

20
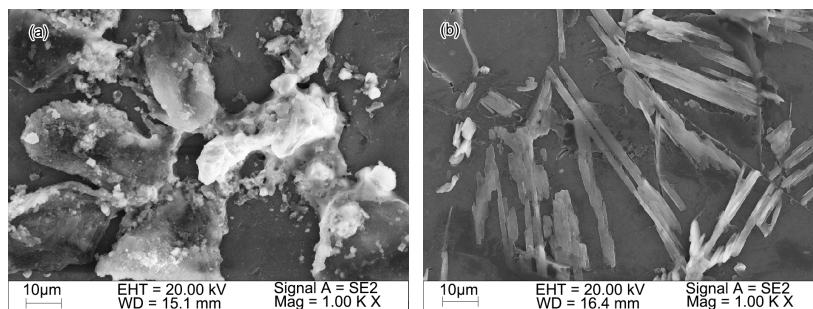
21
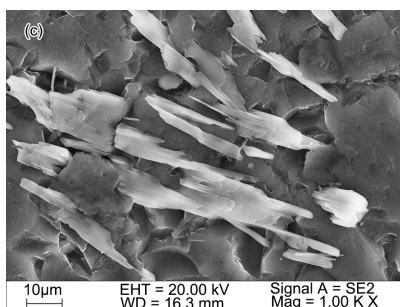
22   Fig. 3. Surface morphology of (a) glycine/GCE, (b) L-cysteine/GCE and (c)

23   L-cysteine/glycine/GCE.

24
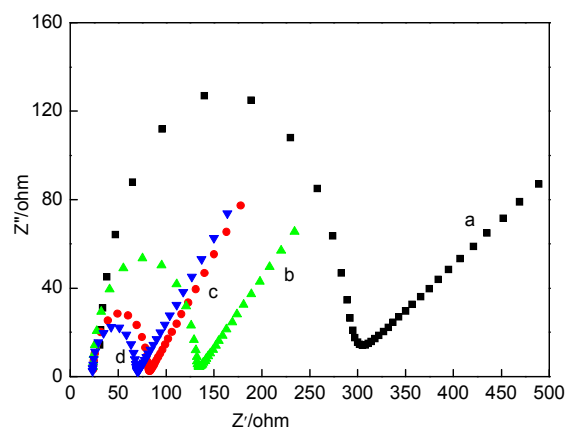
25

26 **Fig. 4.** Nyquist plots of different electrodes in 0.1 M KCl containing 5.0 mM $[Fe(CN)_6]^{3-/4-}$.

27   (a) GCE, (b) Glycine/GCE, (c) L-cysteine/GCE, (d) L-cysteine/glycine/GCE.

28

29
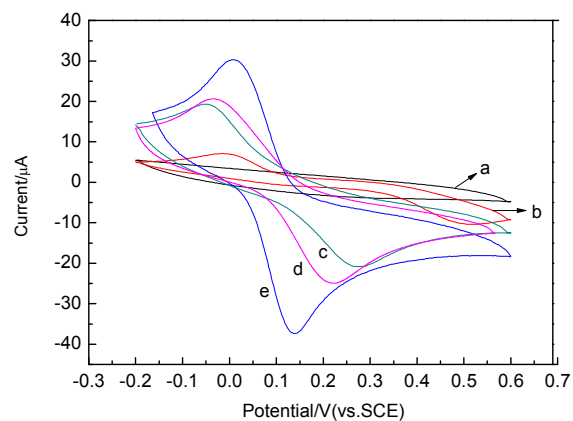
Fig. 5. CV curves of the L-cysteine/glycine/GCE in (a) blank and (e) 50 µM catechol buffer

solution (NaOH-KH$_2$PO$_4$, pH=6.0. (b) - (d) CV curves of the bare GCE, Glycine/GCE, and

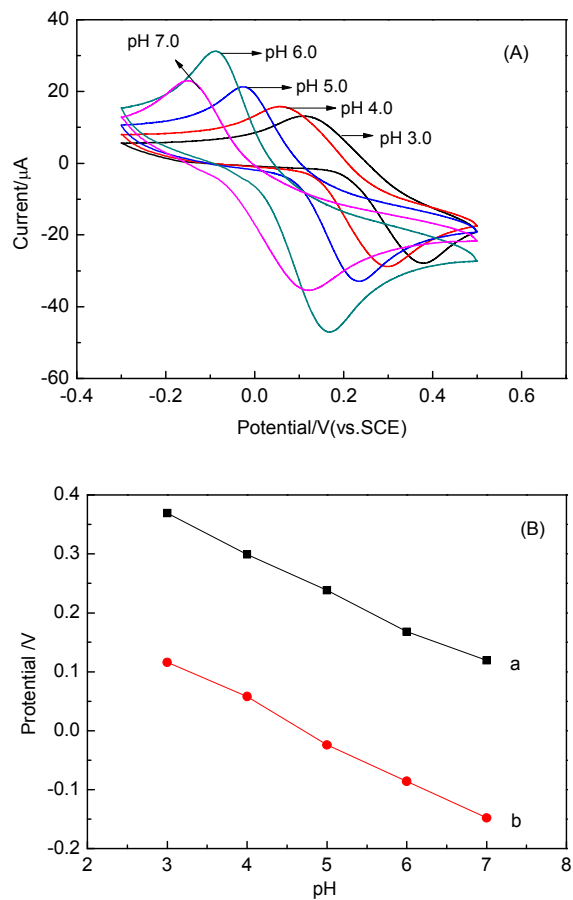L-cysteine/GCE in buffer solution containing 50 µM catechol. The scan rate is 50 mV/s.

35
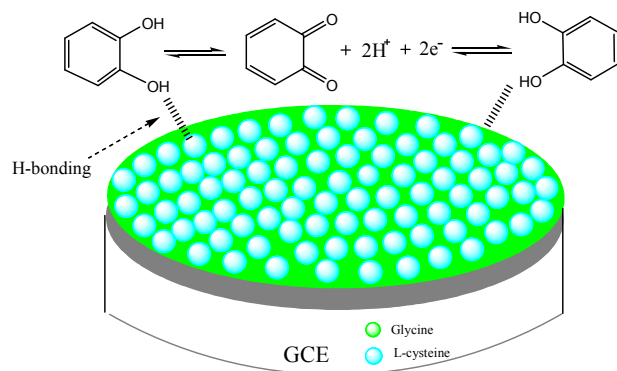
Scheme 4. Schematic illustration of redox reactions of catechol occurring on
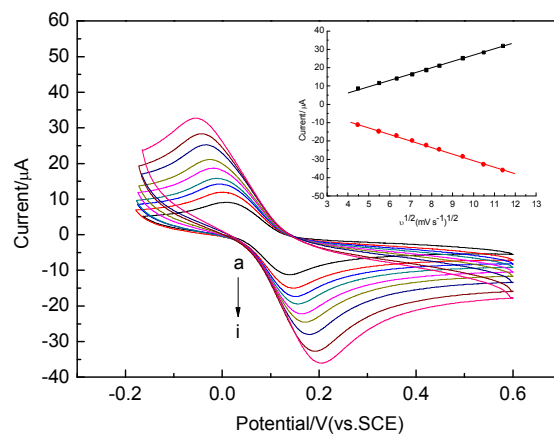
L-cysteine/glycine/GCE.

38

39

40

Fig. 6. (A) CV response of the L-cysteine/glycine/GCE in NaOH-KH$_2$PO$_4$ buffer solution

containing 50 µM catechol of different pH. (B) (a) E$_{pa}$ -pH and (b) E$_{pc}$-pH plots of 50 µM
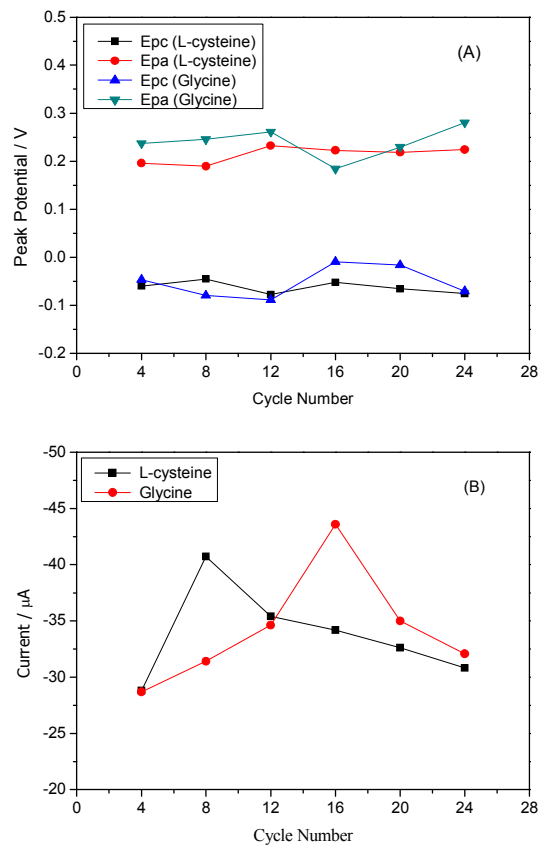
catechol.

45

46

47   **Fig. 7.** Effect of the scan rate on the redox behavior of 50 µM catechol. (a-i) 20, 30, 40, 50,

48   60, 70, 90, 110, 130 mV/s. Inset: the redox peak current of catechol vs. square root of the

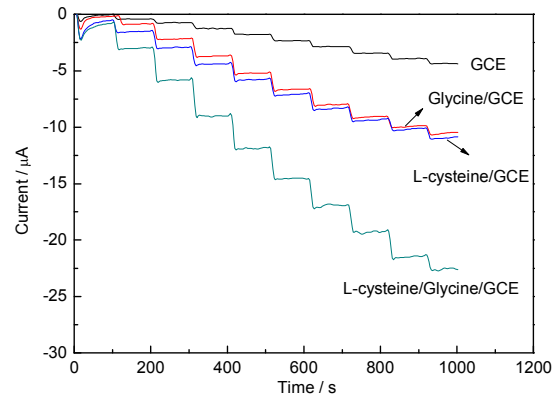49   scan rate.

50

51

52

53

Fig. 8. The variation of the peak potentials (A) and oxidation peak currents (B) for 50

μM catechol in pH 6.0 NaOH-KH_2PO_4 at different cycle numbers of L-cysteine/glycine films

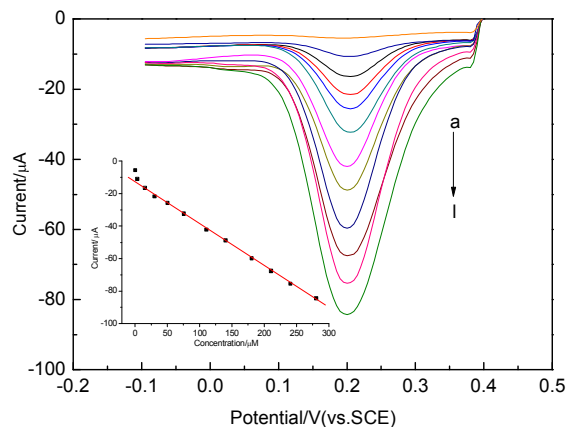modified GCE during the electrodeposition process.

57

58

Fig. 9. Amperometric response of various electrodes to the increase the catechol

concentration (by 10 µM in each step) in buffer solution at the potential of 0.148 V.

61

62

Fig. 10. DPV responses of catechol on the L-cysteine/glycine film electrode at different

catechol concentrations. (a-l: 0, 3, 15, 30, 50, 75, 110, 140, 180, 210, 240, 280 μM). The inset

shows the linear relationship between the oxidation peak current (i_{pa}) and concentration (c).

66

67 **Table 1.** Comparison of different modified electrodes for catechol determination.

Electrodes	Technique	Linear range (μM)	Detection limit (μM)	References
MWNTs-modified electrode	DPV	20-1200	10.0	[43]
AGG/Tyr-modified electrode	DPV	60-800	6.0	[44]
MWCNT-NF-PMG	DPV	360-4050	5.8	[45]
GCE/{Nf-fc}-MME	CV	250-2500	10.8	[46]
CNTEC-Tyr	CV	0-150	10.0	[47]
LDHf/GCE	DPV	3-1500	12.0	[48]
(LDH/HB/LDH/HRP)$_2$	CV	6-170	5.0	[49]
Au-NP/HS(CH$_2$)$_6$SH-Au electrode	CV	4-20	-	[50]
L-cysteine/Glycine/GCE	DPV	3-280	0.32	This study

68

69

70   **Table 2.** Determination of catechol in water samples (n = 6)

Samples	Original concentration of catechol (μM)	Amount of standard catechol added (μM)	Total amount of catechol Found [b] (μM)	Recovery (%)	RSD (%)
1	ND [a]	80.00	79.35	99.2	2.26
2	ND [a]	100.00	102.58	102.6	2.78
3	ND [a]	120.00	120.35	100.3	1.96
4	ND [a]	150.00	151.22	100.8	3.12

71   [a] ND: Not detected.

72   [b] Average of six measurements.

73